Electrical impedance characterization of normal and cancerous human hepatic tissue

2010 Physiol. Meas. 31 995

(http://iopscience.iop.org/0967-3334/31/7/009)

Physiol. Meas. **31** (2010) 995–1009 doi:10.1088/0967-3334/31/7/009

Electrical impedance characterization of normal and cancerous human hepatic tissue

Shlomi Laufer[1], **Antoni Ivorra**[2,3], **Victor E Reuter**[4], **Boris Rubinsky**[1,2,3,6] **and Stephen B Solomon**[5]

[1] Research Center for Bioengineering in the Service of Humanity and Society, School of Computer Science and Engineering, Hebrew University of Jerusalem, Jerusalem, Israel
[2] Department of Bioengineering, University of California, Berkeley, CA, USA
[3] Department of Mechanical Engineering, University of California, Berkeley, CA, USA
[4] Department of Pathology, Memorial Sloan–Kettering Cancer Center, New York, NY, USA
[5] Department of Radiology, Memorial Sloan–Kettering Cancer Center, New York, NY, USA

E-mail: rubinsky@cs.huji.ac.il

Received 28 February 2010, accepted for publication 28 May 2010
Published 24 June 2010
Online at stacks.iop.org/PM/31/995

Abstract

The four-electrode method was used to measure the *ex vivo* complex electrical impedance of tissues from 14 hepatic tumors and the surrounding normal liver from six patients. Measurements were done in the frequency range 1–400 kHz. It was found that the conductivity of the tumor tissue was much higher than that of the normal liver tissue in this frequency range (from 0.14 ± 0.06 S m^{-1} versus 0.03 ± 0.01 S m^{-1} at 1 kHz to 0.25 ± 0.06 S m^{-1} versus 0.15 ± 0.03 S m^{-1} at 400 kHz). The Cole–Cole models were estimated from the experimental data and the four parameters (ρ_0, ρ_∞, α, f_c) were obtained using a least-squares fit algorithm. The Cole–Cole parameters for the cancerous and normal liver are 9 ± 4 Ω m^{-1}, 2.2 ± 0.7 Ω m^{-1}, 0.5 ± 0.2, 140 ± 103 kHz and 50 ± 28 Ω m^{-1}, 3.2 ± 0.6 Ω m^{-1}, 0.64 ± 0.04, 10 ± 7 kHz, respectively. These data can contribute to developing bioelectric applications for tissue diagnostics and in tissue treatment planning with electrical fields such as radiofrequency tissue ablation, electrochemotherapy and gene therapy with reversible electroporation, nanoscale pulsing and irreversible electroporation.

Keywords: bioimpedance, liver cancer

(Some figures in this article are in colour only in the electronic version)

[6] Author to whom any correspondence should be addressed.

Introduction

This study reports new experimental data on the complex electric properties of normal and malignant human liver tissue. Measurement of the electric impedance properties of tissue is not new and the fact that diseased and healthy tissues have different properties is well known and used in medical applications. However, the field of bioengineering in general and bioelectric engineering in particular has an abundance of theoretical or technology papers, but lacks tissue property data—in particular human tissue data. Therefore, it is our belief that any additional measured tissue data are a welcome contribution to the field. Measurements from human tissue are much more difficult to obtain and are more relevant to engineering applications. Several large-scale studies have been published on the electric impedance properties of healthy tissue; perhaps the largest one is that published by Gabriel in 1996 (Gabriel *et al* 1996a, 1996b, 1996c). That study provides data on a large number of various healthy tissues but does not deal with malignant tissues. Furthermore, the lower frequency range (below 1 MHz) was not covered in depth. Gabriel's recent work (Gabriel *et al* 2009) deals with this lower frequency range but once again only for normal tissue. When dealing with cancerous tissue, for which many practical applications of bioelectric engineering exist, these crucial basic data are very sparse or missing. For example, hundreds of papers have been published on EIT (electrical impedance tomography) of the breast. However, to the best of our knowledge, there are only two major studies which report data on the electric properties of human breast cancer tissue (Surowiec *et al* 1988, Jossinet and Schmitt 1999). More comprehensive data on cancer tissue properties would have obvious benefits as regards existing applications. Acquiring such data for the prostate and the breast is currently the focus of the Dartmouth group (Halter *et al* 2009a, 2009b, 2009c). With regard to the liver, there are several new treatments for cancer which require knowledge of the electric properties of liver cancer tissue such as the treatment of cancer by radiofrequency (RF)-induced thermal ablation. In this minimally invasive form of treatment, RF currents (around 400–500 kHz) are injected into the tumor to elevate the temperature through a Joule heating effect to the levels that ablate it (Curley *et al* 1997, Goldberg 2001). Many computer models have been developed to simulate and explore the behavior of electric fields in tumors and normal tissues (Haemmerich *et al* 2003b, Liu *et al* 2005, Chang and Nguyen 2004, Berjano 2006). These models show that the ratio of healthy to malignant tissue electric conductivity has an important influence on the outcome of the treatment (Liu *et al* 2006, Solazzo *et al* 2005). These studies are crucial for understanding and planning RF treatment, but it is all the more concerning to see that the data reported are usually only of healthy tissue. A recent study (Dieter *et al* 2009) is one of the only ones to date to address the issue of the lack of data on malignant tissue, and in this context our independent study has value as adding to the findings of their work. We would like to mention that the general knowledge that the electric properties of cancerous tissue differ from healthy tissue properties is not enough. For example, in the prostate, the malignant tissue has lower electric conductivity than the healthy tissue (Halter *et al* 2009b), whereas in the liver the malignant tissue has higher conductivity.

Our group has two particular reasons for researching the electric properties of cancerous human liver tissue. The first is a new emerging minimally invasive tissue ablation technique called non-thermal irreversible electroporation (NTIRE). In irreversible electroporation, micro- to millisecond high field electric pulses are delivered to undesirable tissue to produce cell necrosis by inducing nanoscale defects in the cell membrane lipid bilayer. In the non-thermal mode, the pulses are designed in such a way as to avoid substantial Joule heating-induced tissue damage due to temperature elevation. Hence NTIRE is a molecular surgery

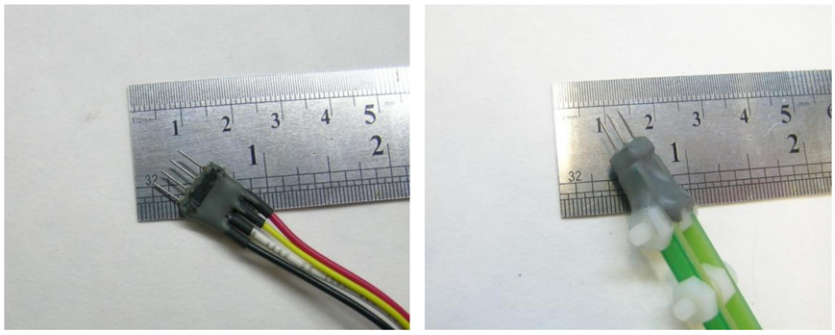

(a) (b)

Figure 1. The four-electrode devices custom made for the experiment. (a) The needles are set in a straight line. (b) The needles are set in a square.

procedure, in the sense that it affects only one molecular component of the tissue—the cell membrane lipid bilayer. Details on the field can be found in a new book (Rubinsky 2010).

Second, we have also developed a classifier-based diagnostic tool based on bioimpedance data. Elsewhere we have shown how bioimpedance can be used to classify tissue types. Although using electric tissue properties for diagnostics is not new, we believe that the classifier-based methods we developed are. It is important to recognize that in developing classifiers a large database of experimental measurements is absolutely essential. Our previous studies on designing classifiers for tissue diagnostics were performed using computer simulations (Laufer and Rubinsky 2009b, Laufer *et al* 2009) or animal models data (with no cancer) (Laufer and Rubinsky 2009a). We used these partial substitutes for actual human tissue data because no relevant human data are available in the literature. In the current study we provide the data needed for developing classifiers. To the best of our knowledge, this work is the first to publish the permittivity (and not just the conductivity) of liver cancer in the reported frequency range. While conductivity is the main property needed for RF and IRE simulations, the complex phase response can be critical when classifying tissue. In our opinion, substantially more studies on human tissue data are needed to further develop the use of classifier techniques in diagnostics.

Materials and methods

EIS measurement

The measurements were performed using the four-electrode method. The electrodes were made from 26 gauge (0.463 mm) hypodermic stainless steel needles. The needles were scratched using sandpaper to maximize their effective area and thus minimize their interface impedance (Geddes 1972). Two types of configurations were made and can be seen in figure 1. In the first configuration, the needles were placed in a straight line with a 2.3 mm distance between the needles and a 5.5 mm exposure. The two outer needles were used for injecting current while the two inner needles were used for measuring the voltage. In the second configuration, the needles were placed in a square shape with a 2.3 mm distance and a 5.5 mm exposure. The two top needles were used for current injection, while the two bottom needles were used for voltage measurement. Although the first configuration gives a better

signal to noise ratio, since the measurement electrodes are in the line of the current electrodes, the second configuration was employed for smaller tumors because of its compact size.

All impedance measurements were performed using a custom-made impedance analyzer embedded in a single printed circuit board (PCB). The impedance analyzer architecture is described in Ivorra and Rubinsky (2007). A total of 11 logarithmically spaced frequencies, ranging from 1 to 400 kHz, were measured. Each scan of all 11 frequencies took 30 ms and each measurement was performed for at least 5 s. The maximum applied current was 100 μAp. The current density calculated from the surface area of the electrode was 1.25 mA cm^{-2} and the RMS value was 0.88 mA cm^{-2}.

Bioimpedance relationships and measurement error evaluation

Bioimpedance is a diagnostic method based on the study of the passive electrical properties of biological tissues. When applying an alternating voltage, V, on a tissue the impedance, Z, is given by the ratio between this voltage and the resulting current, I, namely $V = I \cdot Z$. Alternatively, we can use the admittance value, Y, which is given by $Y = \frac{1}{Z}$. Typically, admittance combines conductive (G) and capacitive (C) components such that $Y = G + \mathrm{j}\omega C$, where $\omega = 2\,\pi\,f$ and j is the complex number $\sqrt{-1}$. G and C depend on the properties of the tissue and on the geometry of the measurement. They are therefore typically separated into two parts:

$$G = K \cdot \sigma \qquad \text{and} \qquad C = K \cdot \varepsilon_0 \varepsilon_r, \tag{1}$$

where σ is the conductivity of the tissue (expressed in S m^{-1}), ε_r is the relative permittivity of the tissue, ε_0 is the permittivity of vacuum (8.85×10^{-12} F m^{-1}) and K is the cell constant, i.e. the geometric scaling factor of the following measurement: cell = area/length (expressed in m^2/m = m). Since G and C are the measured parameters and σ and ε_r are the parameters that characterize the tissue, we first need to evaluate K.

A recent study by Gabriel *et al* (2009), suggested a method to measure the cell constant and evaluate the noise of the measurement. We implemented this method and performed new measurements. The conductance of five NaCl solutions ranging from 0.001 to 0.15 M was measured (this range was chosen since it covers the range of values for the different tissues we studied). Theoretically, ionic solutions such as aqueous NaCl exhibit no dielectric dispersion at frequencies below 1 MHz and the ratio between the conductivities of these different solutions is known. This means that comparison of the different cell constants for different frequencies and different solutions can be used to estimate the total effect of equipment noise and that of different experimental artifacts such as electrode polarization. In this study, we performed such an analysis. The measurements can be seen in figure 2 and the results are summarized in tables 1–3. The method used was the same as that suggested by Gabriel *et al* and a complete description can be found there. The only difference was that we also evaluated the phase data since phase was measured as well. It can be seen that for solutions 0.005–0.15 M, the error was below 9% (compared to 10% in Gabriel *et al*). For 0.001 M a higher error of 23% was present (compared to 67% in Gabriel *et al*), but this solution has very low conductivity, much lower than that of body tissue, and is therefore not relevant to this study. It can also be seen that for the second needle configuration and a concentration of 0.15 M the standard deviation is relatively high (12%). This is due to the fact that the total impedance is less than 10 Ω which is around the limits of our device. Since the liver has higher resistive values, this does not influence this experiment either. The phase of NaCl solutions at these frequencies should be zero and therefore any measured phase can be regarded as an error or artifact (e.g. electrode polarization). In general, the phase was around 2° with the exception of low

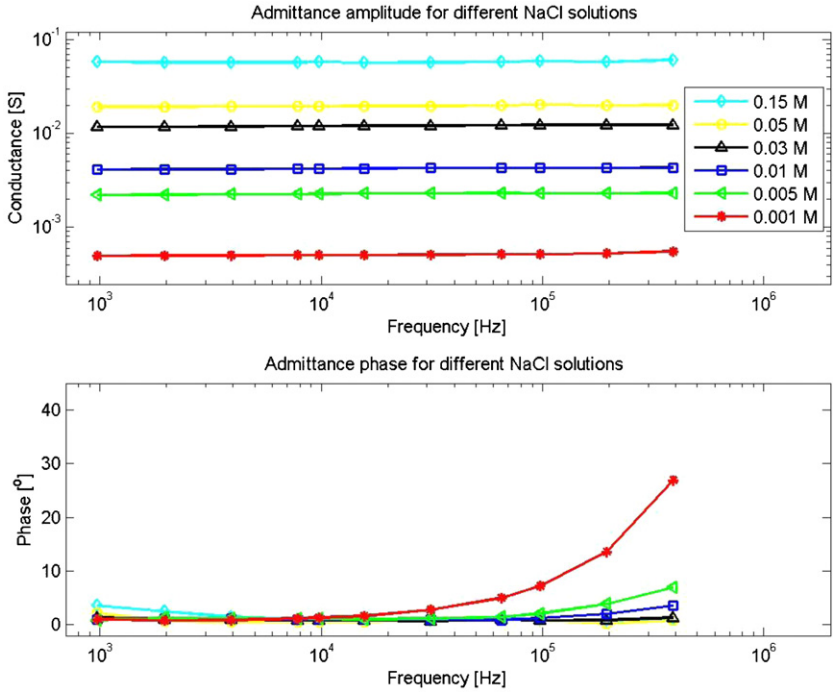

Figure 2. Admittance of different NaCl solutions measured using electrode (a) for cell constant calculation.

NaCl concentration (0.001 M) in the higher frequency range (100–400 kHz). As mentioned, the tissue measured had higher conductivities and consequently this did not influence our measurements.

Tissue handling

This study was approved by the Institutional Review Board (IRB) at the Memorial Sloan–Kettering Cancer Center. All the tissue handling was performed in the Pathology Department under the supervision of one of the hospital pathologists. Measurements were made within 1–2 h of tissue resection. Livers from six patients (three females and three males, four with colon metastases and two with primary liver cancer) with 14 different tumors were examined. The patients were 42–81 year old (average age 58), and the tumor size was between 0.8 and 5 cm (average 2 cm). Of the six livers, one had cirrhosis. Due to the large size of the livers (around 10 cm) and some of the tumors, multiple measurement points were used. A total of 26 points of the healthy liver, 32 points of the cancerous liver and 7 points of the cirrhotic liver were measured. An example of the measurement configuration can be seen in figure 3.

Cole–Cole model fitting

For the parameterization of the frequency-dependent impedance, the Cole–Cole dispersion model (Kenneth and Robert 1941, Jossinet and Schmitt 1999, Halter *et al* 2008) was used, with

$$\rho(f) = \rho_\infty + \frac{\rho_0 - \rho_\infty}{1 + (\mathrm{j}f/f_c)^\alpha}, \tag{2}$$

Table 1. Evaluation of amplitude accuracy. G (S) is the average conductance from 1 to 400 kHz for different NaCl concentrations. The conductivity is calculated using average conductance and the cell constant. The values are given for both electrode configurations (needles in straight line/needles in square).

NaCl (M)	G (S) average	G (S) SD	G (S) % SD	σ (s m^{-1}) average	σ (s m^{-1}) Peyman *et al*	σ (s m^{-1}) difference (%)
0.001	$5.02 \times 10^{-4}/1.03 \times 10^{-3}$	$1.03 \times 10^{-5}/3.01 \times 10^{-5}$	2.05/2.93	0.011/0.012	0.009/0.009	−25.82/−31.29
0.005	$2.26 \times 10^{-3}/4.26 \times 10^{-3}$	$6.87 \times 10^{-5}/1.53 \times 10^{-4}$	3.04/3.59	0.051/0.049	0.047/0.047	−8.42/−4.36
0.01	$4.21 \times 10^{-3}/8.25 \times 10^{-3}$	$9.85 \times 10^{-5}/3.09 \times 10^{-4}$	2.34/3.75	0.095/0.095	0.094/0.094	−0.90/−1.01
0.03	$1.20 \times 10^{-2}/2.30 \times 10^{-2}$	$3.07 \times 10^{-4}/9.04 \times 10^{-4}$	2.55/3.92	0.271/0.265	0.281/0.281	3.51/5.63
0.05	$1.96 \times 10^{-2}/3.90 \times 10^{-2}$	$4.84 \times 10^{-4}/1.81 \times 10^{-3}$	2.48/4.64	0.441/0.449	0.466/0.466	5.38/3.70
0.15	$5.77 \times 10^{-2}/1.18 \times 10^{-1}$	$2.42 \times 10^{-3}/1.50 \times 10^{-2}$	4.20/12.72	1.300/1.355	1.375/1.375	5.48/1.42

Table 2. Evaluation of phase accuracy. The phase average and standard deviation from 1 to 400 kHz for different NaCl concentrations. In this frequency range, the phase should be approximately zero, i.e. the measured phase is due to equipment errors and electrode artifacts and should be minimized. The values are given for both electrode configurations (needles in straight line/needles in square).

NaCl (M)	Phase (°)	Phase (°) SD
0.001	5.66/6.96	7.78/7.89
0.005	2.00/2.79	1.80/1.25
0.01	1.35/2.29	0.78/0.65
0.03	0.95/1.79	0.28/1.26
0.05	0.81/1.69	0.55/2.24
0.15	2.07/6.14	1.43/6.59

Table 3. For NaCl concentrations 0.005–0.15 M and for each frequency, the average percentage of conductivity difference between the data obtained here and the literature and the average phase (which should be zero).

Frequency (Hz)	σ (s m^{-1}) difference (%)	Phase (°)
976.5625	3.30/4.06	1.84/6.66
1953.125	2.85/1.58	1.36/0.68
3906.25	2.38/2.08	1.07/0.44
7812.5	1.70/2.07	0.89/0.73
9765.625	1.58/2.99	0.95/1.06
15 625	1.30/1.61	0.96/1.20
31 250	0.45/1.81	0.90/1.89
65 104	0.05/0.79	1.06/1.97
97 656.25	−0.90/0.40	1.16/1.94
19 5312.5	−0.23/−1.37	1.53/0.35
390 625	−1.39/−4.17	2.69/2.47

where $\rho(f)$ is the complex resistivity given by $\rho = 1/\sigma^*$, where $\sigma^* = \sigma + \mathrm{j}\omega\varepsilon_0\varepsilon_r$, ρ_∞ is the high frequency resistivity, ρ_0 is the low frequency resistivity, f_c is the characteristic frequency, and α is the fractional power representing the depression of the circular arc from the x-axis.

Four parameters (ρ_0, ρ_∞, f_c, α) were estimated with MATLAB's function fsolve using the Levenberg–Marquardt method. As in Halter *et al* (2008), the quality of the estimation was evaluated using the goodness criterion:

$$\varepsilon = \frac{1}{N}\sum_{i=1}^{N} |\rho_m(f_i) - \rho_e(f_i)|, \tag{3}$$

where $\rho_m(f_i)$ and $\rho_e(f_i)$ are the measured and estimated impedances at each frequency, respectively, and N is the number of frequencies (in our case 11).

The initial parameters were set in the following manner (Halter *et al* 2008):

ρ_∞: real part of impedance at the maximum frequency, 400 kHz.
ρ_0: real part of impedance at the minimum frequency, 1 kHz.
f_c: frequency at which $\mathrm{Im}(\rho_m(f_i)) > \mathrm{Im}(\rho_m(f_{i-1}))$ and $\mathrm{Im}(\rho_m(f_i)) > \mathrm{Im}(\rho_m(f_{i+1}))$ first occur as the frequency proceeds from low to high $i = 2, 3, \ldots, N-1$.
α: set to 1 for all cases.

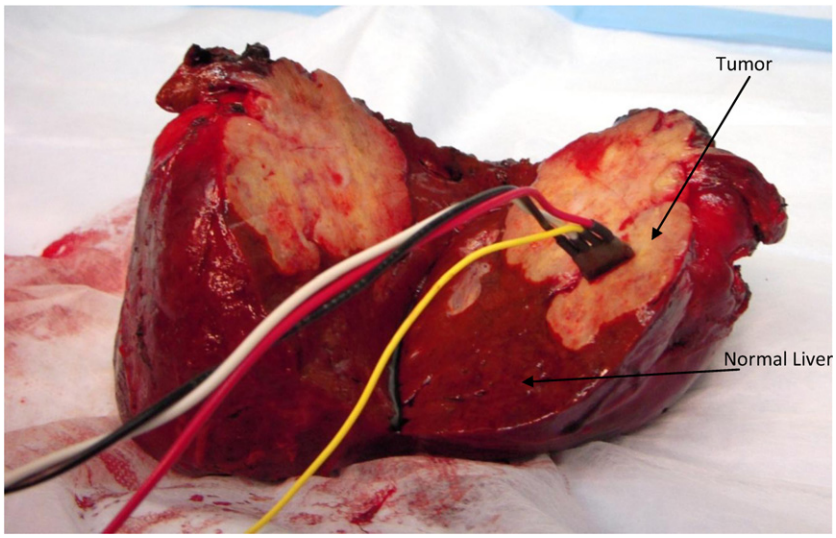

Figure 3. Example of the measurement configuration.

Results

When presenting bioimpedance data using the matching Cole–Cole models, two approaches can be taken. In the first approach the impedance values from all the tissue data sets are initially averaged and then these average values are used to extract the Cole–Cole parameters. In the second approach a Cole–Cole model is developed for each tissue data set and the model parameters are averaged over all the data sets. Due to variations between tissues these two methods yield different results. Furthermore, while the first method gives the standard deviation of the impedance values, in the second method the standard deviation is of the Cole–Cole parameters. Averaging the impedance values has the advantages of averaging the data that were actually measured and avoiding the model fitting stage, which is known to introduce errors. When examining the correlation between the different impedance values for different frequencies, we found them to be much higher ($\sim$0.9) than those of different Cole–Cole parameters ($\sim$0.45). This would suggest that when adding independent and identically distributed (i.i.d) noise to simulated data (for example in computer models), it would be better to use the Cole–Cole model and add the noise to Cole–Cole parameters and not to the impedance values. Given these considerations we decided to present the Cole–Cole parameters obtained from both methods. The average and standard deviation of the electrical conductivity and the relative permittivity can be found in table 4 and are plotted in figure 4. As a reference, the data for a normal liver from Gabriel *et al* (1996b) are also presented in figure 4. The average impedance values can be seen in figure 5 and the average admittance in figure 6. The Cole–Cole parameters were also calculated for each of the measurements. The average error between the model and the measured data was $0.1 \pm 0.1\ \Omega$ (approximately 1%). A sample of these models can be seen in figure 7, and the average and standard deviation are presented in table 5.

Table 4. Average conductivity and permittivity of normal, cancerous and cirrhotic tissues.

Frequency (Hz)	Normal conductivity (S m^{-1})	Tumor conductivity (S m^{-1})	Cirrhotic conductivity (S m^{-1})	Normal relative permittivity	Tumor relative permittivity	Cirrhotic relative permittivity
976.6	0.030 ± 0.01	0.166 ± 0.08	0.105 ± 0.02	$8.2\times10^4 \pm 2\times10^4$	$9.9\times10^4 \pm 6\times10^4$	$1\times10^5 \pm 1\times10^4$
1953.1	0.032 ± 0.01	0.169 ± 0.08	0.107 ± 0.02	$6.6\times10^4 \pm 2\times10^4$	$8\times10^4 \pm 4\times10^4$	$7.4\times10^4 \pm 6\times10^3$
3906.3	0.035 ± 0.01	0.173 ± 0.08	0.110 ± 0.02	$5.2\times10^4 \pm 1\times10^4$	$5.8\times10^4 \pm 2\times10^4$	$5.9\times10^4 \pm 3\times10^3$
7812.5	0.040 ± 0.01	0.179 ± 0.08	0.116 ± 0.02	$3.8\times10^4 \pm 9\times10^3$	$3.9\times10^4 \pm 1\times10^4$	$4.5\times10^4 \pm 2\times10^3$
9765.6	0.042 ± 0.01	0.181 ± 0.08	0.119 ± 0.02	$3.5\times10^4 \pm 8\times10^3$	$3.4\times10^4 \pm 1\times10^4$	$4\times10^4 \pm 2\times10^3$
15 625.0	0.047 ± 0.01	0.185 ± 0.08	0.125 ± 0.02	$2.8\times10^4 \pm 7\times10^3$	$2.5\times10^4 \pm 7\times10^3$	$3.2\times10^4 \pm 1\times10^3$
31 250.0	0.058 ± 0.02	0.195 ± 0.07	0.138 ± 0.02	$2^4 \pm 5\times10^3$	$1.6\times10^4 \pm 5\times10^3$	$2.2\times10^4 \pm 1\times10^3$
65 104.0	0.076 ± 0.02	0.209 ± 0.07	0.155 ± 0.02	$1.3\times10^4 \pm 3\times10^3$	$1\times10^3 \pm 3\times10^3$	$1.3\times10^4 \pm 7\times10^2$
97 656.3	0.091 ± 0.02	0.222 ± 0.07	0.176 ± 0.02	$1.1\times10^4 \pm 2\times10^3$	$8.6\times10^3 \pm 2\times10^3$	$1.1\times10^4 \pm 5\times10^2$
195 312.5	0.124 ± 0.03	0.246 ± 0.07	0.208 ± 0.01	$6.5\times10^3 \pm 1\times10^3$	$5.1\times10^3 \pm 1\times10^3$	$6.2\times10^3 \pm 3\times10^2$
390 625.0	0.164 ± 0.03	0.272 ± 0.07	0.244 ± 0.01	$3.4\times10^3 \pm 5\times10^2$	$3\times10^3 \pm 6\times10^2$	$3.2\times10^3 \pm 2\times10^2$

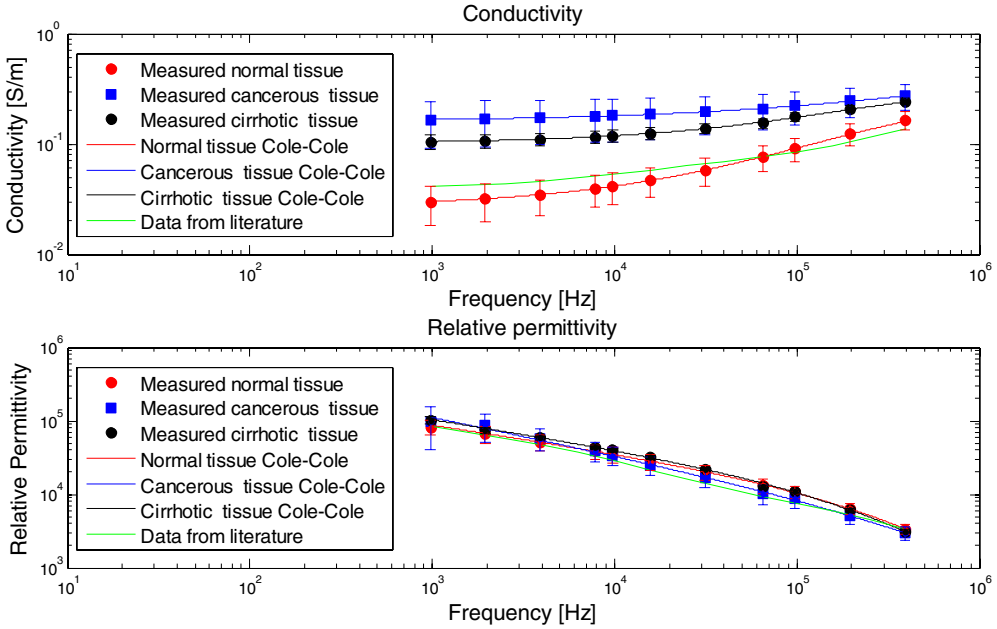

Figure 4. Average conductivity and permittivity of normal, cancerous and cirrhotic tissues. As a reference, data from the literature are presented (Andreuccetti *et al* 1997, Gabriel *et al* 1996b). The continuous lines are the Cole–Cole model fits for these data with the following parameters: normal tissue, $\rho_0 = 37.26$ (Ω m), $\rho_\infty = 3.31$ (Ω m), $\alpha = 0.634$, $f_c = 9358$ (Hz); cancerous tissue, $\rho_0 = 6.23$ (Ω m), $\rho_\infty = 1.94$ (Ω m), $\alpha = 0.503$, $f_c = 144\,731$ (Hz); cirrhotic tissue, $\rho_0 = 9.9$ (Ω m), $\rho\infty = 2.76$ (Ω m), $\alpha = 0.62$, $f_c = 41752$ (Hz).

Discussion

Previous studies of a liver, both animal and human (Smith *et al* 1986, Joines *et al* 1994, Haemmerich *et al* 2003a, Stauffer *et al* 2003, O'Rourke *et al* 2007, Dieter *et al* 2009), showed that cancerous tissue has higher conductivity values than healthy tissue. In our study, we found the same relationship. These ratios are not trivial since in prostate cancer the tumor has lower conductivity than the surrounding healthy tissue (Halter *et al* 2008, 2009c), while in breast cancer the tumor has higher conductivity than the surrounding fat typically found at older ages, but lower than glandular tissue (Jossinet and Schmitt 1999).

It has also been found that the difference in electrical conductivity values is much higher in the lower frequency range, as reported in Dieter *et al* (2009). In Haemmerich and Wood (2006) and Dieter *et al* (2009), it was suggested that the RF ablation frequency (currently around 400–500 kHz) should be reduced. It was shown that although the conductivity of malignant tissue is higher at all frequencies, the difference is much higher at lower frequencies and therefore performing the ablation process at lower frequencies will cause the current to preferentially heat the malignant tissue. This will cause better destruction of the tumor with less damage to surrounding tissue. Further studies should examine impedance values on the border of the tumor. If they are closer to those of healthy tissue, then reducing the frequency might accelerate the necrosis of the center of the tumor, where lower conductivities exist, while leaving the boundary alive to regenerate. Another issue is that the difference between ablated tissue and non-ablated tissue is much higher at the lower frequency range (Dieter

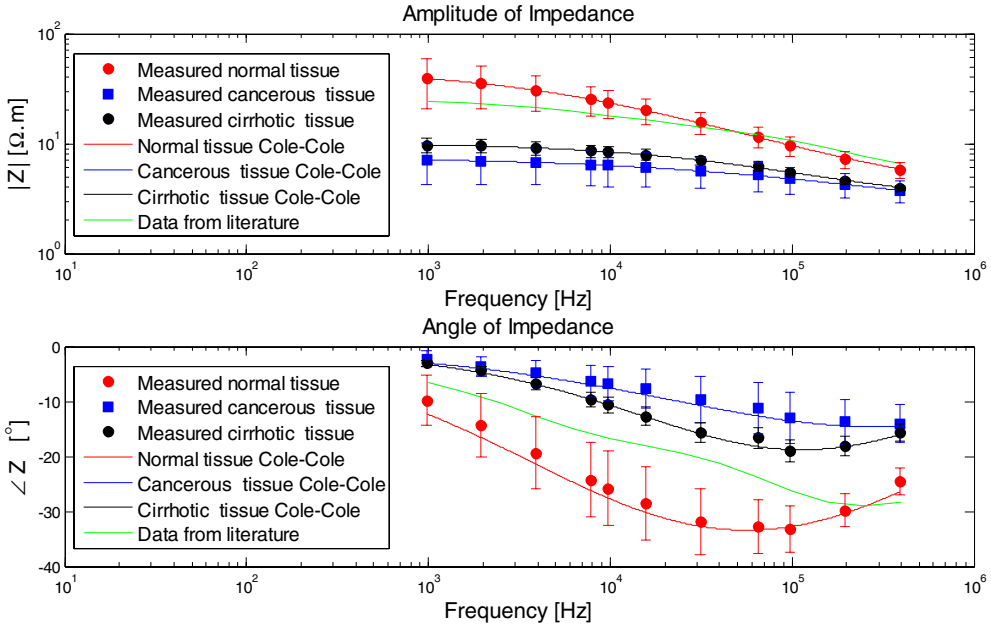

Figure 5. Average impedance amplitude and angle of normal, cancerous and cirrhotic tissues. As a reference, data from the literature are presented (Andreuccetti *et al* 1997, Gabriel *et al* 1996b). The continuous lines are the Cole–Cole model fits for these data with the following parameters: normal tissue, $\rho_0 = 47.96$ (Ω m), $\rho_\infty = 3.06$ (Ω m), $\alpha = 0.594$, $f_c = 5567$ (Hz); cancerous tissue, $\rho_0 = 7.54$ (Ω m), $\rho_\infty = 2.04$ (Ω m), $\alpha = 0.492$, $f_c = 82\,294$ (Hz); cirrhotic tissue, $\rho_0 = 10.14$ (Ω m), $\rho_\infty = 2.76$ (Ω m), $\alpha = 0.617$, $f_c = 39\,682$ (Hz).

et al 2009). Once again this can encourage the electrical currents and the resulting heating to concentrate in the ablated area where the electrical conductivity is higher. Although using higher frequencies seems less efficient, the heating process might be more homogenous and thus more predictable. These parameters should be used in future computer simulations, and more *ex vivo* RF ablation experiments should be performed for a better understanding of the problem.

In addition, it was seen that the β dispersion central frequency of the malignant tissue was much higher than that of the normal tissue (155.7 kHz and 10.5 kHz, respectively). The β dispersion depends on the cell membrane capacity. Since regions of cell necrosis are commonly found inside tumor tissue, the capacitive effect of the intact cell membrane in those areas is reduced. As mentioned, the conductivity at the lower frequency range is much higher in cancerous tissue. This could be due to higher extra-cellular water content in the tumor and lower cell membrane density due to necrosis. At the high frequency range the conductivity is still higher, although less significant than in the lower range, and this would suggest intracellular changes as well.

Only one liver was cirrhotic, and thus further studies need to be done. The conductivity of this liver was much higher than that of the healthy liver and it had a reduced phase response in comparison to healthy tissue. The considerable difference between healthy and cirrhotic liver could suggest bioimpedance as a method for non-invasive liver evaluation (using methods similar to electrical impedance tomography).

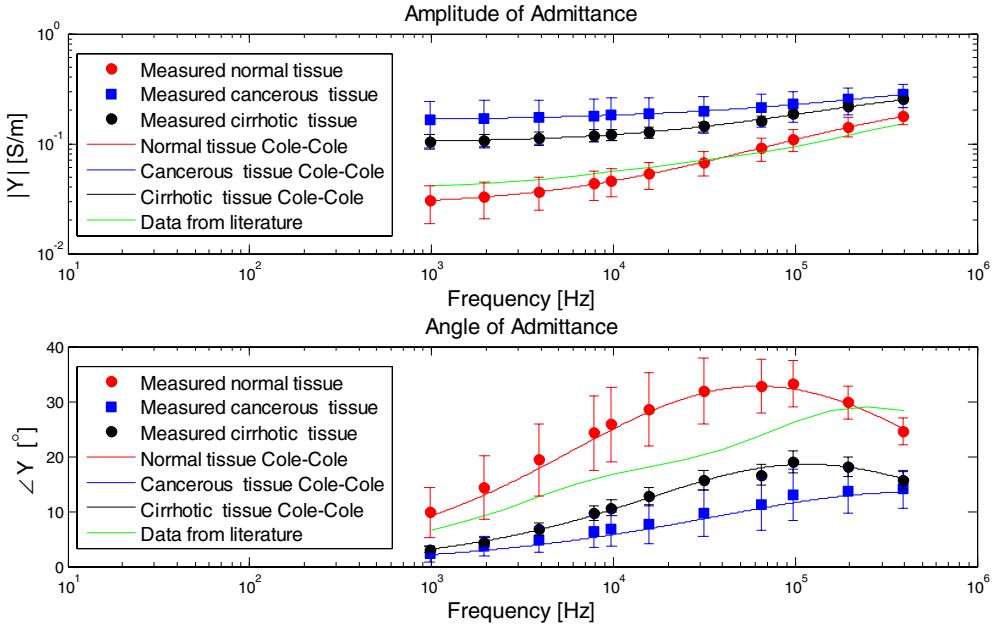

Figure 6. Average admittance amplitude and angle of normal, cancerous and cirrhotic tissues. As a reference, data from the literature are presented (Andreuccetti *et al* 1997, Gabriel *et al* 1996b). The continuous lines are the Cole–Cole model fits for these data with the same parameters as in figure 4.

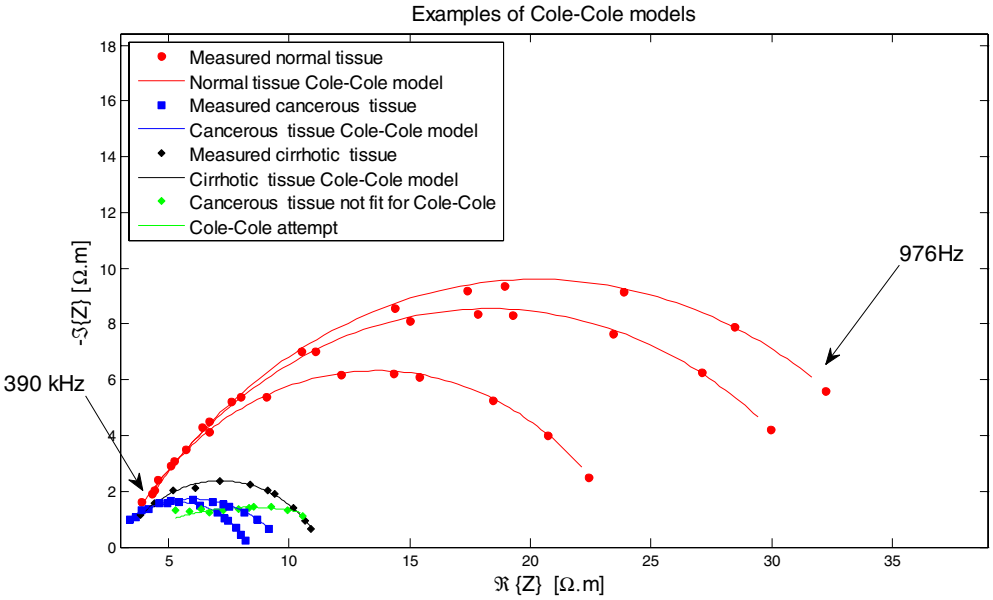

Figure 7. Examples of the Cole–Cole models of different tissues.

Table 5. Average of the Cole–Cole parameters.

Parameters	Units	Normal	Tumor	Cirrhotic
ρ_0	(Ω m)	47.58 ± 28.94	7.56 ± 3.44	10.14 ± 1.66
ρ_∞	(Ω m)	3.29 ± 0.65	2.15 ± 0.72	2.76 ± 0.14
α	–	0.63 ± 0.04	0.51 ± 0.14	0.62 ± 0.02
f_c	(kHz)	10.5 ± 7	155.7 ± 132	41.5 ± 8

Another interesting fact was that while for all the healthy tissues a Cole–Cole model was easily fit, the frequency response for some of the cancerous tissue was 'flat' and thus the model appeared not to fit. This phenomenon has been reported in previous studies (Antoni *et al* 2009, Jossinet and Schmitt 1999) and an example can be seen in figure 7. This could influence the relatively large variability of parameter f_c in the Cole–Cole model.

The wide variability of the data in this study is a disturbing matter. We found the variability to be around 25% for healthy tissue and 40% for cancerous tissue, while the consistency of our equipment was better than 9% and on average around 5%. However, large variability is not unusual and has been reported in other studies as well (Halter *et al* 2009b, Jossinet and Schmitt 1999). A possible explanation can be found in Haemmerich *et al* (2002) which shows that the conductivity in an animal model decreases by 53% at 10 Hz and by 32% at 1 MHz during the first 2 h after liver removal. Since in a clinical setup we cannot control the exact time between removal of the liver and the time when the tissue properties are measured, this can influence the variability of the data, as was pointed out by Halter *et al* (2009b). The effect of the time lag on measurement observed by Haemmerich *et al* coincides to some extent with the fact that in our data the variability was higher at the lower frequency range. This variability in the lower frequency range, especially in permittivity, could also be due to electrode polarization which is more dominant in this frequency range. In four of the livers, we measured more than four areas and we calculated the standard deviation. We found it to be 15% for healthy tissue and 25% for cancerous tissue. Since these measurements were performed approximately at the same time, this suggests that these values represent the measurement accuracy and tissue inhomogeneity, whereas the remainder can be ascribed to patient variability and the time lag between tissue extraction and measurement. The larger variability in tumors is probably due to their irregular form. It was also shown in Haemmerich *et al* (2002) that after 24 h the conductivity values rise again. This could explain why on average we obtained lower values than those found by Gabriel *et al* (1996b). The variability in the data further emphasizes the need for many more experimental studies on physiological measurements of human tissue data for bioimpedance applications. Further studies should also examine whether the time of ischemia affects differently malignant and normal liver tissue.

Conclusion

The electrical conductivity and permittivity of *ex vivo* malignant and healthy liver tissue were measured. It was found that malignant tissue had higher conductivity values and a lower phase response in the entire measured frequency range (1–400 kHz). These data can be used for both bioimpedance needle guidance and improving the RF ablation procedure. In this work, we did not distinguish between different types of liver cancers due to the small amount of data and IRB constraints. This should be examined in larger samples, and the feasibility of using bioimpedance measurements as a classifier should be evaluated. Furthermore, it

would be interesting to compare malignant tumors to benign tumors; these data could be used to construct bioimpedance-based tissue classifiers (Laufer and Rubinsky 2009a, 2009b). Examining the homogeneity of impedance values over the entire tumor, including its borders, could help improve the RF ablation procedure.

References

Andreuccetti D, Fossi R and Petrucci C 1997 Calculation of the dielectric properties of body tissues in the frequency range 10 Hz–100 GHz (Florence: IFAC-CNR) http://niremf.ifac.cnr.it/tissprop/

Antoni I *et al* 2009 *In vivo* electrical conductivity measurements during and after tumor electroporation: conductivity changes reflect the treatment outcome *Phys. Med. Biol.* **54** 5949

Berjano E J 2006 Theoretical modeling for radiofrequency ablation: state-of-the-art and challenges for the future *Biomed. Eng. Online* **5** 24

Chang I A and Nguyen U D 2004 Thermal modeling of lesion growth with radiofrequency ablation devices *Biomed. Eng. Online* **3** 27

Curley S A, Davidson B S, Fleming R Y, Izzo F, Stephens L C, Tinkey P and Cromeens D 1997 Laparoscopically guided bipolar radiofrequency ablation of areas of porcine liver *Surg. Endosc.* **11** 729–33

Dieter H *et al* 2009 Electrical conductivity measurement of excised human metastatic liver tumours before and after thermal ablation *Physiol. Meas.* **30** 459

Gabriel C, Gabriel S and Corthout E 1996a The dielectric properties of biological tissues: I. Literature survey *Phys. Med. Biol.* **41** 2231–49

Gabriel C, Peyman A and Grant E H 2009 Electrical conductivity of tissue at frequencies below 1 MHz *Phys. Med. Biol.* **54** 4863–78

Gabriel S, Lau R W and Gabriel C 1996b The dielectric properties of biological tissues: II. Measurements in the frequency range 10 Hz to 20 GHz *Phys. Med. Biol.* **41** 2251–69

Gabriel S, Lau R W and Gabriel C 1996c The dielectric properties of biological tissues: III. Parametric models for the dielectric spectrum of tissues *Phys. Med. Biol.* **41** 2271–93

Geddes L A 1972 *Electrodes and the Measurement of Bioelectric Events* (New York: Wiley-Interscience)

Goldberg S N 2001 Radiofrequency tumor ablation: principles and techniques *Eur. J. Ultrasound* **13** 129–47

Haemmerich D, Ozkan R, Tungjitkusolmun S, Tsai J Z, Mahvi D M, Staelin S T and Webster J G 2002 Changes in electrical resistivity of swine liver after occlusion and postmortem *Med. Biol. Eng. Comput.* **40** 29–33

Haemmerich D, Staelin S T, Tsai J Z, Tungjitkusolmun S, Mahvi D M and Webster J G 2003a *In vivo* electrical conductivity of hepatic tumours *Physiol. Meas.* **24** 251–60

Haemmerich D and Wood B J 2006 Hepatic radiofrequency ablation at low frequencies preferentially heats tumour tissue *Int. J. Hyperth.* **22** 563–74

Haemmerich D, Wright A W, Mahvi D M, Lee F T Jr and Webster J G 2003b Hepatic bipolar radiofrequency ablation creates coagulation zones close to blood vessels: a finite element study *Med. Biol. Eng. Comput.* **41** 317–23

Halter R J *et al* 2009a The correlation of *in vivo* and *ex vivo* tissue dielectric properties to validate electromagnetic breast imaging: initial clinical experience *Physiol. Meas.* **30** S121–36

Halter R J, Hartov A, Paulsen K D, Schned A and Heaney J 2008 Genetic and least squares algorithms for estimating spectral EIS parameters of prostatic tissues *Physiol. Meas.* **29** S111–23

Halter R J, Schned A, Heaney J, Hartov A and Paulsen K D 2009b Electrical properties of prostatic tissues: I. Single frequency admittivity properties *J. Urol.* **182** 1600–7

Halter R J, Schned A, Heaney J, Hartov A and Paulsen K D 2009c Electrical properties of prostatic tissues: II. Spectral admittivity properties *J. Urol.* **182** 1608–13

Ivorra A and Rubinsky B 2007 *In vivo* electrical impedance measurements during and after electroporation of rat liver *Bioelectrochemistry* **70** 287–95

Joines W T, Zhang Y, Li C and Jirtle R L 1994 The measured electrical properties of normal and malignant human tissues from 50 to 900 MHz *Med. Phys.* **21** 547–50

Jossinet J and Schmitt M 1999 A review of parameters for the bioelectrical characterization of breast tissue *Ann. NY Acad. Sci.* **873** 30–41

Kenneth S C and Robert H C 1941 Dispersion and absorption in dielectrics: I. Alternating current characteristics *J. Chem. Phys.* **9** 341–51

Laufer S and Rubinsky B 2009a Cellular phone enabled non-invasive tissue classifier *PLoS ONE* **4** e5178

Laufer S and Rubinsky B 2009b Tissue characterization with an electrical spectroscopy SVM classifier *IEEE Trans. Biomed. Eng.* **56** 525–8

Laufer S, Solomon S B and Rubinsky B 2009 A new linear algebra based mathematical technique for electrical impedance spectroscopy guided biopsy *World Congress on Medical Physics and Biomedical Engineering (Munich, Germany, 7–12 September 2009)* pp 583–6

Liu Z, Ahmed M, Weinstein Y, Yi M, Mahajan R L and Goldberg S N 2006 Characterization of the RF ablation-induced 'oven effect': the importance of background tissue thermal conductivity on tissue heating *Int. J. Hyperth.* **22** 327–42

Liu Z, Lobo S M, Humphries S, Horkan C, Solazzo S A, Hines-Peralta A U, Lenkinski R E and Goldberg S N 2005 Radiofrequency tumor ablation: insight into improved efficacy using computer modeling *Am. J. Roentgenol.* **184** 1347–52

O'Rourke A P, Lazebnik M, Bertram J M, Converse M C, Hagness S C, Webster J G and Mahvi D M 2007 Dielectric properties of human normal, malignant and cirrhotic liver tissue: *in vivo* and *ex vivo* measurements from 0.5 to 20 GHz using a precision open-ended coaxial probe *Phys. Med. Biol.* **52** 4707–19

Rubinsky B 2010 Irreversible electroporation *Series in Biomedical Engineering* (Berlin: Springer) pp X1V, 314

Smith S R, Foster K R and Wolf G L 1986 Dielectric properties of VX-2 carcinoma versus normal liver tissue *IEEE Trans. Biomed. Eng.* **33** 522–4

Solazzo S A, Liu Z, Lobo S M, Ahmed M, Hines-Peralta A U, Lenkinski R E and Goldberg S N 2005 Radiofrequency ablation: importance of background tissue electrical conductivity—an agar phantom and computer modeling study *Radiology* **236** 495–502

Stauffer P R, Rossetto F, Prakash M, Neuman D G and Lee T 2003 Phantom and animal tissues for modelling the electrical properties of human liver *Int. J. Hyperth.* **19** 89–101

Surowiec A J, Stuchly S S, Barr J R and Swarup A A S A 1988 Dielectric properties of breast carcinoma and the surrounding tissues *Biomed. Eng., IEEE Trans.* **35** 257–63